

π -Hole $\cdots d_z^2$ [Pt^{II}] Interactions with Electron-Deficient Arenes Enhance the Phosphorescence of Pt^{II}-Based Luminophores

Anton V. Rozhkov, Ivan V. Ananyev, Rosa M. Gomila, Antonio Frontera,* and Vadim Yu. Kukushkin*

Cite This: <https://dx.doi.org/10.1021/acs.inorgchem.0c01170>

Read Online

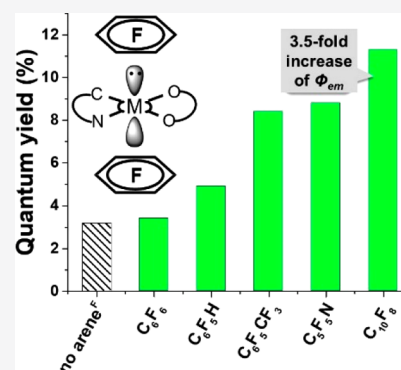
ACCESS |

Metrics & More

Article Recommendations

Supporting Information

ABSTRACT: Two phosphorescent Pt^{II}-based cyclometalated complexes were co-crystallized with perfluorinated arenes to give 1:1 co-crystals. The X-ray study revealed that each of the complexes is embraced by arenes^F to give infinite reverse sandwich structures. In four out of six structures, a d_z^2 orbital of Pt^{II} is directed to the arenes^F ring via π -hole $\cdots d_z^2$ [Pt^{II}] interactions, whereas in the other two structures, the filled d_z^2 orbital is directed toward the arene C atoms. Computed molecular electrostatic potential surfaces of the arenes^F and the complexes, noncovalent interaction indexes for the co-crystals, and natural bond orbital calculations indicate that π -hole $\cdots d_z^2$ [Pt^{II}] contacts (and, generally, the stacking) are of electrostatic origin. The solid-state photophysical study revealed up to 3.5-fold luminescence quantum yield and 15-fold lifetime enhancements in the co-crystals. This increase is associated with the strength of the π -hole $\cdots d_z^2$ [Pt^{II}] contact that is dependent on the π -acidity of the arene^F and its spatial characteristics.



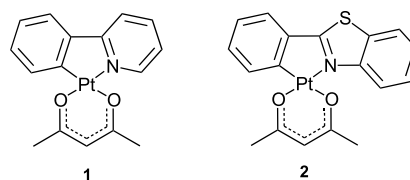
INTRODUCTION

In the past decade, rational manipulation of noncovalent interactions involving σ -hole (σh) or π -hole (πh) donors has proven to be an efficient method to design luminescent materials and modulate their photophysical properties.^{1–4} Some σh -involved interactions in co-crystals of purely organic or metal-containing luminescent materials provide room-temperature phosphorescence instead of fluorescence (observed in the absence of appropriate noncovalent contacts)⁵ and substantial enhancement of luminescence quantum yields^{6,7} (up to a 20-fold halogen bonding-assisted increase has been detected⁶), and these interactions can also modify emission spectra.⁸

The modulation of luminescent properties by noncovalent interactions involving π -hole (πh) donors is another useful strategy in the design of organic luminescent materials,^{9–12} although it is incomparably less common than the modulation via σh interactions. To the best of our knowledge, *enhancement* of the luminescence of any metal-containing system by πh interactions has never been observed in the past. We report herein on the increase of phosphorescence quantum yields of luminescent systems based on Pt^{II} square-planar cyclometalated complexes **1** and **2** (see Figure 1). This effect is achieved by their co-crystallization with electron-deficient arenes to give infinite reverse sandwich structures,¹³ including $\pi h\cdots d_z^2$ [Pt^{II}] contacts.

RESULTS AND DISCUSSION

Previously, we reported¹³ that square-planar platinum(II) and palladium(II) systems co-crystallize with πh -donating electron-deficient arene systems, giving a family of reverse sandwich

Figure 1. Parent luminophores **1** and **2**.

species. The latter are based on $\pi h\cdots d_z^2$ [M^{II}] interactions when the charge distribution at the metal center and at the arenes is opposite to that of the classic sandwiches, and the positively charged d^8 -M center acts as a nucleophile.¹⁴ For this work, we addressed platinum(II) complexes **1** and **2** exhibiting pronounced phosphorescent properties (for **1**, $\Phi_{em} = 15\%$ and $\mu = 2.60 \mu s$ in 2-MeTHF;¹⁵ for **2**, $\Phi_{em} = 36\%$ and $\mu = 0.34 \mu s$ in CH₂Cl₂¹⁶), obtained their co-crystals with electron-deficient arenes and a hetarene, and compared phosphorescent properties of **1** and **2** with those of the corresponding co-crystals.

The complex [Pt(ppy)acc] (**1**, where ppyH = 2-phenylpyridine and Hacac = acetylacetonate)¹⁷ co-crystallizes with the arenes (C₆F₆, C₆F₅H, C₆F₅CF₃), pentafluoropyridine (C₅F₅N) as hetarene, and octafluoronaphthalene (C₁₀F₈) at 20–25 °C

Received: April 22, 2020

to give, in each case, 1:1 co-crystals $1 \cdot (\text{arene}^{\text{F}})$, while the diketone complex $[\text{Pt}(\text{bt})\text{acac}]$ (**2**, where $\text{btH} = 2$ -phenylbenzothiazole)¹⁸ form 1:1 co-crystals $2 \cdot \text{C}_{10}\text{F}_8$ with octafluoronaphthalene; our attempts to obtain co-crystals of **2** with the remaining arenes^F were unsuccessful.

All six co-crystals were studied using X-ray diffraction (XRD), and their packing (see Figures S1–S6 in the Supporting Information) consist of alternating layers of the complexes and the arenes^F. The main motif of regular parallel arrangement of a planar complex and arenes^F is mostly induced by weak $\text{CH} \cdots \text{F}$ contacts within layers and moderate $\pi \cdots \pi$ stacking interlayer interactions (see Figures S1–S4). The exception is isostructural $1 \cdot \text{C}_6\text{F}_6$ and $1 \cdot \text{C}_6\text{F}_5\text{H}$ co-crystals (see Figures S5 and S6), where this regular architecture of the stacking-bonded layers is affected by $\text{CH} \cdots \text{F}$ and $\text{CH} \cdots \pi$ interlayer interactions. This variation of the crystal packings provides differences in the supramolecular environment of the metal site. In $1 \cdot \text{C}_6\text{F}_5\text{CF}_3$, $1 \cdot \text{C}_5\text{F}_5\text{N}$, $1 \cdot \text{C}_{10}\text{F}_8$, and $2 \cdot \text{C}_{10}\text{F}_8$ (see Figure 2, as well as Figures S7–S9 in the Supporting

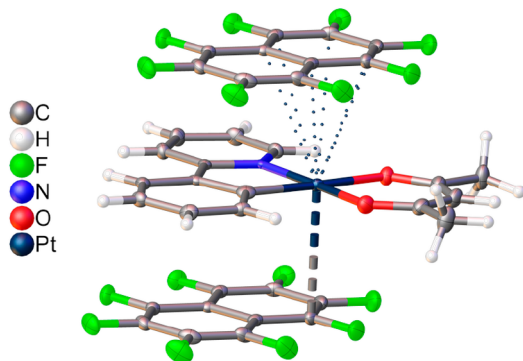


Figure 2. Molecular structure of $1 \cdot \text{C}_{10}\text{F}_8$ with dashed short contacts. Non-hydrogen atoms are given as probability ellipsoids of atomic displacements ($p = 0.5$).

Information), the Pt atom from both sides is enclosed by two perfluoroarenes, whereas in $1 \cdot \text{C}_6\text{F}_6$ and $1 \cdot \text{C}_6\text{F}_5\text{H}$ (Figures S10 and S11 in the Supporting Information), only one arene^F directly contacts the metal centers, whereas another one is significantly shifted toward the (acac)Pt moiety. The asymmetry of $\pi \cdots \text{Pt}$ interaction in these two co-crystals could cause their specific crystal packing, as indicated above.

The geometry of these arene^F \cdots Pt contacts supports the availability of the metal-involving stacking interactions. The angle between mean-square planes of any one of the metal complexes and a perfluoroarene is $< 2^\circ$, while the distance between the Pt atom and the arene^F plane (3.274(6)–3.357(4) Å, see also Table S1 in the Supporting Information for other structural details) is always less than the sum of Bondi van der Waals radii (R_{vdW}) for C and Pt (3.45 Å). Despite these conservative geometric features, the specifics of $\pi \cdots \text{Pt}$ interaction, namely, the direction of the Pt d_z^2 orbital, with respect to arene^F, are dependent on the identity of perfluoroarene (Figure 3). If in $1 \cdot \text{C}_6\text{F}_5\text{CF}_3$, $1 \cdot \text{C}_5\text{F}_5\text{N}$, $1 \cdot \text{C}_{10}\text{F}_8$, and $2 \cdot \text{C}_{10}\text{F}_8$, the d_z^2 orbital is directed to the ring (one ring for C_{10}F_8) favoring $\pi \text{h} \cdots d_z^2[\text{Pt}^{\text{II}}]$ interaction,¹³ in $1 \cdot \text{C}_6\text{F}_6$ and $1 \cdot \text{C}_6\text{F}_5\text{H}$, the filled d_z^2 orbital is shifted from the rings toward C atoms.

For $1 \cdot \text{C}_6\text{F}_6$ and $1 \cdot \text{C}_6\text{F}_5\text{H}$ co-crystals, only one rather strong $\text{C} \cdots \text{Pt}$ interaction can be assumed (3.316(5) and 3.347(5) Å, respectively) and the other $\text{C} \cdots \text{Pt}$ distances with arenes^F are

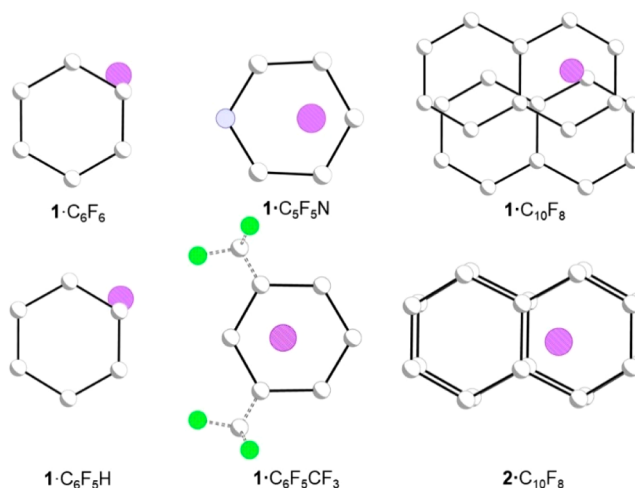


Figure 3. Projections of Pt centers (shown in purple) onto the mean-square planes of the closest aromatic rings in the studied co-crystals. For co-crystal $1 \cdot \text{C}_6\text{F}_5\text{CF}_3$, two possible CF_3 positions (due to symmetry-imposed disorder) are given by double-dashed lines.

significantly longer (3.477(5)–4.375(5) and 3.575(5)–4.427(6) Å, respectively). The formation of weaker—but still short $\text{C} \cdots \text{Pt}$ contacts (3.405(6) Å) between the Pt center and two opposite $\text{C}_5\text{F}_5\text{N}$ in $1 \cdot \text{C}_5\text{F}_5\text{N}$ —results in more symmetric $\pi \cdots \text{Pt}$ interactions ($\text{N} \cdots \text{Pt} = 3.750(6)$ Å, $\text{C} \cdots \text{Pt} = 3.405(6)$ – $3.651(6)$ Å). This trend is even more pronounced in $1 \cdot \text{C}_6\text{F}_5\text{CF}_3$, where the metal center is not involved in any specific $\text{C} \cdots \text{Pt}$ contact and the $\text{C} \cdots \text{Pt}$ distances with the C_6F_5 ring of two $\text{C}_6\text{F}_5\text{CF}_3$ are in the narrow range (3.547(5)–3.694(5) Å).

Finally, the most symmetric $\pi \cdots \text{Pt}$ interaction was found in $1 \cdot \text{C}_{10}\text{F}_8$ (the $\text{C} \cdots \text{Pt}$ distances with the closest C_6 ring of the two neighboring arenes^F vary from 3.563(4) Å to 3.678(4) Å). However, in comparison with the other co-crystals of **1**, this system combines both $\pi \cdots \text{Pt}$ interaction modes, i.e., while the Pt atom provides its d_z^2 orbital for the symmetric $\pi \cdots \text{Pt}$ interaction, it is also involved in the shortened $\text{C} \cdots \text{Pt}$ contact with the opposite C_{10}F_8 (3.382(4) Å). A similar but more uniform bonding situation was found in $2 \cdot \text{C}_{10}\text{F}_8$: the $\text{C} \cdots \text{Pt}$ distances of more symmetric $\pi \cdots \text{Pt}$ interaction cover a 0.299 Å range, which is noticeably wider than that in $1 \cdot \text{C}_{10}\text{F}_8$. In contrast, the $\text{C} \cdots \text{Pt}$ range of distances for the more directional $\pi \cdots \text{Pt}$ interaction is smaller in $2 \cdot \text{C}_{10}\text{F}_8$ (0.411 Å) with the formally shortened contact $\text{C} \cdots \text{Pt}$ being comparable to the R_{vdW} sum (3.443(7) Å vs 3.45 Å).

The molecular electrostatic potential (MEP) surfaces of the arenes^F and compounds **1** and **2** have been represented in Figures 4 and 5, respectively. Despite the fact that the Mulliken atomic charge densities at the Pt atom in **1** and **2** are positive (0.36 and 0.38 e, respectively), the MEP plotted onto the van der Waals surfaces of these two complexes reveal the existence of a large isosurface of negative potential over the Pt^{II} center and the phenyl ring is directly bonded. The MEP values over the pyridine ring in **1** or the benzothiazole ring in **2** are significant less electron-rich. The MEP value over the central C atom of the acac ligand is also negative (−13 kcal/mol in both compounds). The most π -acidic arenes^F are $\text{C}_5\text{F}_5\text{N}$ and $\text{C}_6\text{F}_5\text{CF}_3$, and the less acidic arene is $\text{C}_6\text{F}_5\text{H}$. Both C_6F_6 and C_{10}F_8 exhibit similar MEP values over the center of the rings. This analysis indicates a good complementary situation between the arenes^F with π -acidic surfaces and **1** and **2** with

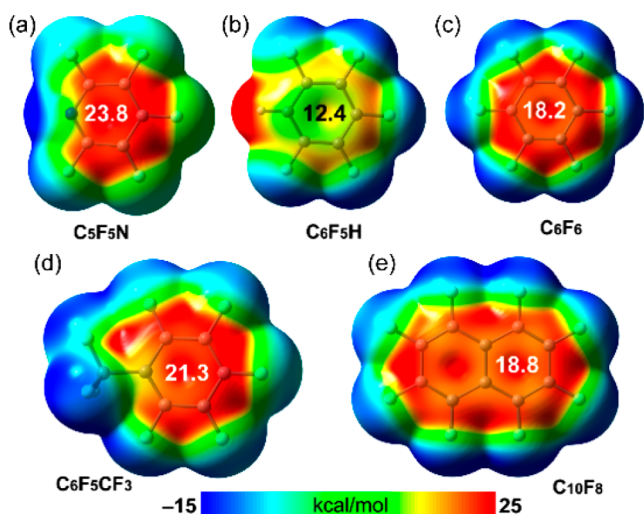


Figure 4. MEP surfaces (0.001 a.u.) of the perfluoroarenes at the PBE1PBE-D3/def2-TZVP level of theory: (a) C_5F_5N , (b) C_6F_5H , (c) C_6F_6 , (d) $C_6F_5CF_3$, and (e) $C_{10}F_8$. The energies over the ring centroids are given in kcal/mol. [Color code: blue = negative, red = positive.]

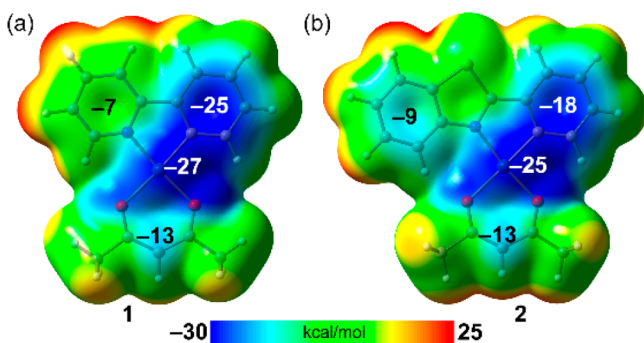


Figure 5. MEP surfaces (0.001 a.u.) of (a) **1** and (b) **2** used in this work at the PBE1PBE-D3/def2-TZVP level of theory. [Color code: blue = negative, red = positive.]

large π -basic surfaces embracing the Pt^{II} center. Therefore, electrostatic forces are very important for the formation of the ternary assemblies commented above.

To further characterize the π -stacking interactions, we have used the NCIPLOT computational tool. It can be defined as a computational index that is very convenient for the easy visualization and identification of noncovalent interactions. These are identified with the peaks that emerge in the reduced density gradient (RDG) at low densities.^{19,20} These are visualized by mapping an isosurface of s ($s = |\nabla\rho|/\rho^{4/3}$) for a low value of RDG. When a supramolecular assembly is formed, the RDG changes at the critical points (CP) located between the monomers due to the annihilation of the density gradient at these CPs. Therefore, the NCIPLOT index reveals which molecular regions interact. Moreover, it also provides qualitative information about the attractive or repulsive nature of the interaction. That is, red and yellow colors are indicative of strong and weak repulsive forces (ρ_{cut}^+), respectively, and blue and green colors correspond to strong and weak attractive forces (ρ_{cut}^-), respectively.

The representation for all ternary assemblies are given in Figure 6, along with their interaction energies computed at the PBE1PBE-D3/def2-TZVP level of theory (the interaction

energies are calculated between two aromatic molecules and the Pt-complex **1** or **2**). The energetic results show a qualitative good agreement with the MEP surfaces. That is, the weakest complex corresponds to $1 \cdot C_6F_5H$, followed by $1 \cdot C_6F_6$, which are the aromatic rings with smallest values of MEP. Complexes $1 \cdot C_5F_5N$ and $1 \cdot C_6F_5CF_3$ present stronger interactions, because of its higher π -acidity and also the presence of the CF_3 group in $1 \cdot C_6F_5CF_3$ that likely contributes to reinforce the interaction through some long-range contacts with the methyl groups of the acac ligand. In fact, there is an excellent correlation between the interaction energies and the MEP values for co-crystals $1 \cdot C_6F_5H$, $1 \cdot C_6F_6$, and $1 \cdot C_5F_5N$ ($r^2 = 0.986$). However, $1 \cdot C_6F_5CF_3$ does not follow the same trend, thus confirming the extra stabilization gained due to presence the CF_3 groups. Finally, $1 \cdot C_{10}F_8$ and $2 \cdot C_{10}F_8$ exhibit the strongest interactions, because of the larger overlap of the π -systems.

The NCIPLOT index shows the existence of extended green isosurfaces located between the π -systems in all trimers, thus confirming the attractive nature of the interaction. Moreover, the extension of the surfaces in $1 \cdot C_{10}F_8$ and $2 \cdot C_{10}F_8$ confirms the large complementarity in these systems. The $\pi h \cdots d_z^2 [Pt^{II}]$ interaction is characterized by a concave isosurface that is generated between the Pt^{II} center and the aromatic π -cloud of the arenes^F. These isosurfaces are observed in all complexes apart from the weakest $1 \cdot C_6F_5H$ and $1 \cdot C_6F_6$, where the interaction is better defined as $(FC=CF) \cdots d_z^2 [Pt^{II}]$ that is characterized by the presence of small isosurfaces (see Figures 6b and 6c). Interestingly, the strongest complexes $1 \cdot C_5F_5N$ and $1 \cdot C_6F_5CF_3$ (6-membered rings) and $2 \cdot C_{10}F_8$ (two fused rings) show the concave surfaces above and below the Pt^{II} center, thus forming two simultaneous $\pi h \cdots d_z^2 [Pt^{II}]$ interactions. $1 \cdot C_{10}F_8$ exhibits a $\pi h \cdots d_z^2 [Pt^{II}]$ interaction on one side and $(FC=CF) \cdots d_z^2 [Pt^{II}]$ on the opposite side, thus likely explaining its weaker interaction energy compared to $2 \cdot C_{10}F_8$.

The correspondence between the π -acidity of the rings (MEP surfaces) and the interaction energies of the ternary complexes suggests that the interaction is dominated by electrostatic effects (electron-rich Pt^{II} and π -acidic electron-deficient arenes^F). Nevertheless, we have also studied if orbital contributions are important in the $\pi h \cdots d_z^2 [Pt^{II}]$ bonding interactions described above. To accomplish it, we have performed natural bond orbital (NBO) calculations, focusing on the second-order perturbation analysis that is adequate to analyze donor–acceptor interactions.²¹ Remarkably, this analysis reveals that the orbital contributions in all trimers are moderate, as summarized in Table 1. For each fluoroarene in the complexes (above and below the Pt complex), we have found two complementary contributions: (i) an electron donation ($5d_z^2(Pt) \rightarrow \pi^*$) from the d_z^2 at the Pt atom to π -antibonding orbitals of the arene and (ii) a back-donation from π -bonding orbitals of the arene to the empty $6p_z$ atomic orbital of Pt. While the overall orbital contribution is higher for the back-donation (Table 1), the energies are modest, compared to the total interaction energy. Therefore, taking into consideration the MEP surface analysis, interaction energies and $E^{(2)}$ orbital donor–acceptor energies, it can be concluded that the interaction can be better defined as $\pi h \cdots d_z^2 [Pt^{II}]$ bonding interaction dominated by electrostatic forces with a moderate contribution from an orbital back-donation (up to 2.34 kcal/mol in $2 \cdot C_{10}F_8$, see Table 1) from the π -system of the fluoroarene to the empty $6p_z$ atomic orbital of Pt.

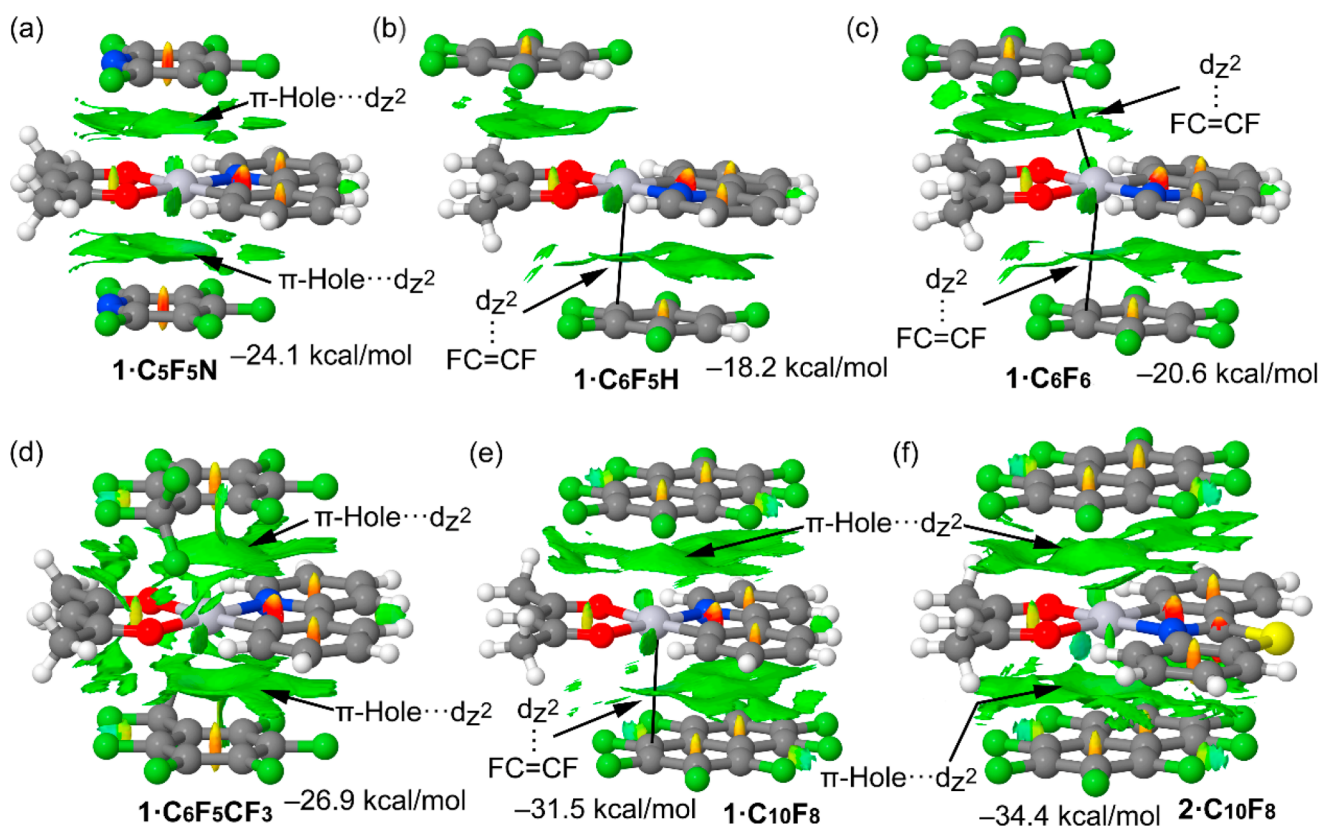


Figure 6. NCIplots of (a) $1 \cdot C_5F_5N$, (b) $1 \cdot C_6F_5H$, (c) $1 \cdot C_6F_6$, (d) $1 \cdot C_6F_5CF_3$, (e) $1 \cdot C_{10}F_8$, and (f) $2 \cdot C_{10}F_8$. The interaction energies of the ternary assemblies at the PBE1PBE-D3/def2-TZVP level of theory are shown. The parameters used to build the surface are a gradient cutoff of 0.35 a.u. and a color scale of -0.04 a.u. $< \rho < 0.04$ a.u.

The photophysical properties of **1** and **2** and their co-crystals (see Table S2 in the Supporting Information) have been studied in the solid state. The solid-state emission spectra of **1** and **2**, and all of their co-crystals (see Figure 7, as well as Figure S12 in the Supporting Information), are broad, partially structured, and, in accordance with ref 22, could be attributed to a mixture of $^3LLC/CT$ and 3MLCT transitions. The phosphorescence is characterized by $\tau_{obs} = 0.28$ – $8.42 \mu s$, which is attributed to the triplet manifold (see Table S2). As can be inferred from the inspection of Table S2, co-crystallization with the πh donors lead to up to 3.5-fold increase of Φ_{em} for all co-crystals and up to 14.5-fold lifetimes; the profile of the spectra changes insignificantly.

The most significant alterations of the phosphorescence, as compared to **1** and **2**, were observed in perfluoronaphthalene co-crystals (1 and 2)· $C_{10}F_8$; ca. 3.5-fold Φ_{em} and excited-state lifetimes enhancement was achieved for $1 \cdot C_{10}F_8$ (11.3%; $8.42 \mu s$) vs **1** (Φ_{em} 3.2%; $0.58 \mu s$). In addition, we observed a substantial change in the profile of the emission spectrum of the adduct vs **1** (see Figure S12); the bands in $1 \cdot C_{10}F_8$ are better resolved and structured and the shortwave band becomes more intense (see Figure 7a). For $2 \cdot C_{10}F_8$, we did not observe a significant increase in Φ_{em} , compared to **2**: Φ_{em} 16.5% (**2**) and 18.8% ($2 \cdot C_{10}F_8$). In contrast, ca. 4-fold τ_{obs} enhancement was detected ($\tau_{obs} = 0.95 \mu s$ (**2**) and $\tau_{obs} = 3.88 \mu s$ ($2 \cdot C_{10}F_8$)). The profile of the emission spectrum of $2 \cdot C_{10}F_8$ vs **2** (Figure 7b), as for **1**, underwent the same changes. We assume that co-crystallization prevents intermolecular interaction to diminish nonradiative decay via excimer formation²³ and also increases the structural rigidity of **1** and **2**, preventing

the rotational/vibrational motion of the luminescent moiety and suppressing the nonradiative decays; all of these lead to Φ_{em} enhancement and structuring the emission spectra. However, to start a comprehensive photophysical study supporting this assumption, more experimental examples are required for co-crystals of the complexes with arenes exhibiting extended conjugated π -systems equal to or larger than that in perfluoronaphthalene.

Notably, in the context of this work, the only metal-containing luminescent system—whose phosphorescence is affected by πh contacts with electron-deficient organic species—is based on highly nucleophilic²⁴ d^{10} -[Au^I₃] clusters; co-crystallization of these species with, e.g., $C_{10}F_8$ to give [Au^I₃]/ $C_{10}F_8$ associates exhibiting $\pi h \cdots d_{z^2}[\text{metal}]$ short contacts completely quenches the luminescence of the parent clusters.^{25–27}

We believe that the enhancement of the phosphorescence of **1** and **2**, upon the interaction with the arenes^F, is associated with the strength and spatial features of the appropriate interactions, namely, the efficiency of the overlapping of the πh and a $d_{z^2}[\text{Pt}^{\text{II}}]$ orbital (recall Figure 3) or, in the other words, the interaction energy between perfluoroarenes and the complexes (recall Table 1). The observed changes in the quantum yield and the profile of the emission spectrum correlate well with the degree of shielding of Pt^{II} by arenes^F (the isolation of the complex from each other) and the stacking interaction energy (Table 1). Our further works in this direction will be focused on the stacking of metal-based square-planar luminophores and species exhibiting substantially extended aromatic systems with deep πh .

Table 1. Orbital Donor–Acceptor Interactions in the Ternary π – π Complexes of 1 and 2 at the PBE1PBE-D3/def2-TZVP Level of Theory^a

compound	donor	acceptor	$E^{(2)}$ (kcal/mol)
1-C ₆ F ₆	$5d_z^2(\text{Pt})$	$\pi^*(\text{C}_6\text{F}_6)$	0.57
	$5d_z^2(\text{Pt})$	$\pi^*(\text{C}_6\text{F}_6)$	0.14
	$\pi(\text{C}_6\text{F}_6)$	$6p_z^2(\text{Pt})$	2.01
	$\pi(\text{C}_6\text{F}_6)$	$6p_z^2(\text{Pt})$	1.03
1-C ₆ F ₅ H	$5d_z^2(\text{Pt})$	$\pi^*(\text{C}_6\text{F}_5\text{H})$	0.06
	$5d_z^2(\text{Pt})$	$\pi^*(\text{C}_6\text{F}_5\text{H})$	0.89
	$\pi(\text{C}_6\text{F}_5\text{H})$	$6p_z^2(\text{Pt})$	2.37
	$\pi(\text{C}_6\text{F}_5\text{H})$	$6p_z^2(\text{Pt})$	1.25
1-C ₆ F ₅ CF ₃	$5d_z^2(\text{Pt})$	$\pi^*(\text{C}_6\text{F}_5\text{CF}_3)$	0.07
	$5d_z^2(\text{Pt})$	$\pi^*(\text{C}_6\text{F}_5\text{CF}_3)$	0.07
	$\pi(\text{C}_6\text{F}_5\text{CF}_3)$	$6p_z^2(\text{Pt})$	1.49
	$\pi(\text{C}_6\text{F}_5\text{CF}_3)$	$6p_z^2(\text{Pt})$	1.49
1-C ₅ F ₅ N	$5d_z^2(\text{Pt})$	$\pi^*(\text{C}_5\text{F}_5\text{N})$	0.31
	$5d_z^2(\text{Pt})$	$\pi^*(\text{C}_5\text{F}_5\text{N})$	0.31
	$\pi(\text{C}_5\text{F}_5\text{N})$	$6p_z^2(\text{Pt})$	1.37
	$\pi(\text{C}_5\text{F}_5\text{N})$	$6p_z^2(\text{Pt})$	1.37
1-C ₁₀ F ₈	$5d_z^2(\text{Pt})$	$\pi^*(\text{C}_{10}\text{F}_8)$	0.07
	$5d_z^2(\text{Pt})$	$\pi^*(\text{C}_{10}\text{F}_8)$	1.83
	$\pi(\text{C}_{10}\text{F}_8)$	$6p_z^2(\text{Pt})$	3.52
	$\pi(\text{C}_{10}\text{F}_8)$	$6p_z^2(\text{Pt})$	1.50
2-C ₁₀ F ₈	$5d_z^2(\text{Pt})$	$\pi^*(\text{C}_{10}\text{F}_8)$	1.49
	$5d_z^2(\text{Pt})$	$\pi^*(\text{C}_{10}\text{F}_8)$	1.52
	$\pi(\text{C}_{10}\text{F}_8)$	$6p_z^2(\text{Pt})$	2.03
	$\pi(\text{C}_{10}\text{F}_8)$	$6p_z^2(\text{Pt})$	2.34

^aContributions corresponding to back-donation are shown in italic font.

EXPERIMENTAL SECTION

Materials. Pt(ppy)acac²⁸ and Pt(bt)ppy¹⁸ were synthesized using published methods. Hexafluorobenzene, pentafluorobenzene, octafluorotoluene, pentafluoropyridine, and octafluoronaphthalene were purchased from Sigma–Aldrich Chemical Co. and used as received.

X-ray Diffraction Studies. XRD experiments were performed with Xcalibur and Supernova diffractometers, using Cu K α radiation (graphite or mirror monochromators, ω -scans) at 100 K. The structures were solved by direct method and refined by the full-matrix least-squares against F₂ in anisotropic approximation for non-hydrogen atoms. All hydrogen-atom positions were calculated. All hydrogen atoms were refined in isotropic approximation in the riding model. The equal substitution disorder model was used for the C and N atoms connected with a Pt atom. Crystal data and structure refinement parameters are given in Table S3 in the Supporting Information. All calculations were performed using the SHELX software.²⁹ CCDC Data File Nos. 1996567–1996572 contain all additional supplementary data.

Computational Details. The energies of the complexes included in this study were computed at the PBE1PBE-D3/def2-TZVP level of theory by using the Gaussian-16 program.³⁰ The interaction energy (or binding energy in this work), ΔE , is defined as the energy difference between the trimer complex and the sum of the energies of the monomers. The basis set superposition error has been corrected using the counterpoise method.³¹ For the calculations, we have used the Weigend def2-TZVP^{32,33} basis set and the PBE1PBE DFT functional.^{34,35} Grimme's D3 dispersion correction has been used^{36,37} to better estimate the π – π interactions. The molecular electrostatic potential (MEP) surface calculations have been computed using

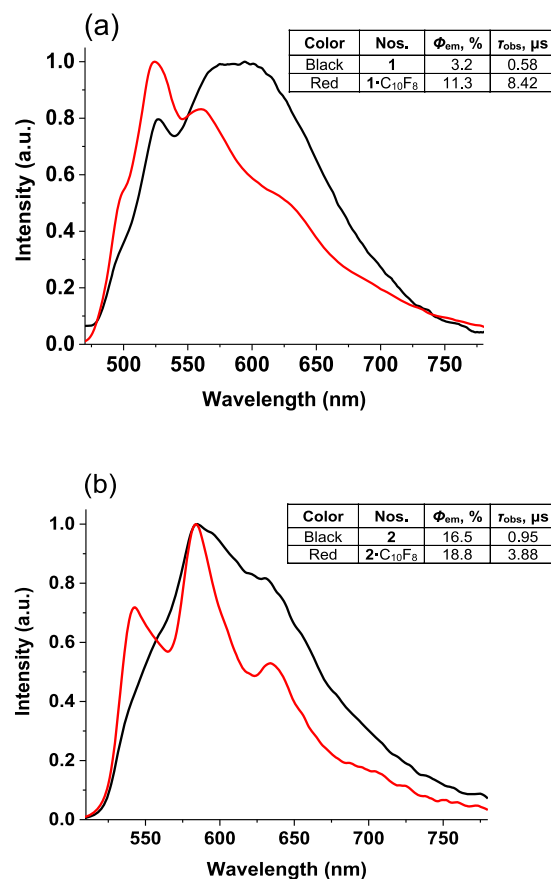


Figure 7. Normalized solid-state emission spectra of (a) 1 (1-C₁₀F₈) and (b) 2 (2-C₁₀F₈) at 298 K; $\lambda_{\text{exit.}} = 405$ nm.

Gaussian-16 software at the PBE1PBE-D3/def2-TZVP level of theory. The NCIPLLOT^{19,20} index has been performed using the PBE1PBE-D3/def2-TZVP wave function.

Crystal Growth. The single crystals were prepared via the slow evaporation of solutions of 1 and 2 in the fluorinated arenes (ca. 5 mg of any one of the complexes in 3 mL of a fluorinated arene) and slow evaporation of CH₂Cl₂ solutions containing equimolar amounts of 1 and 2 and octafluoronaphthalene at 20–25 °C.

ASSOCIATED CONTENT

Supporting Information

The Supporting Information is available free of charge at <https://pubs.acs.org/doi/10.1021/acs.inorgchem.0c01170>.

Additional figures and tables (PDF)

Accession Codes

CCDC 1996567–1996572 contain the supplementary crystallographic data for this paper. These data can be obtained free of charge via www.ccdc.cam.ac.uk/data_request/cif, or by emailing data_request@ccdc.cam.ac.uk, or by contacting The Cambridge Crystallographic Data Centre, 12 Union Road, Cambridge CB2 1EZ, UK; fax: +44 1223 336033.

AUTHOR INFORMATION

Corresponding Authors

Antonio Frontera – Department of Chemistry, Universitat de les Illes Balears, 07122 Palma de Mallorca, Balears, Spain;

orcid.org/0000-0001-7840-2139; Email: toni.frontera@uib.es

Vadim Yu. Kukushkin – Institute of Chemistry, Saint Petersburg State University, 199034 Saint Petersburg, Russia;
orcid.org/0000-0002-2253-085X; Email: v.kukushkin@spbu.ru

Authors

Anton V. Rozhkov – Institute of Chemistry, Saint Petersburg State University, 199034 Saint Petersburg, Russia;
orcid.org/0000-0002-8658-7281

Ivan V. Ananyev – A. N. Nesmeyanov Institute of Organoelement Compounds of RAS, 119991 Moscow, Russia;
orcid.org/0000-0001-6867-7534

Rosa M. Gomila – Department of Chemistry, Universitat de les Illes Balears, 07122 Palma de Mallorca, Balears, Spain

Complete contact information is available at:

<https://pubs.acs.org/10.1021/acs.inorgchem.0c01170>

Author Contributions

The manuscript was written through contributions of all authors. All authors have given approval to the final version of the manuscript. A.V.R. and V.Y.K. conceived the project. A.V.R. synthesized the complexes and their adducts, measured the luminescent spectra, analyzed the data, and wrote the article. I.V.A. performed the X-ray study and wrote the crystallographic part. R.M.G. and A.F. performed the quantum chemical calculations and wrote the theoretical part. V.Y.K. supervised this project and edited the text of the article.

Funding

Funding from the Russian Science Foundation (No. 19-73-00052) is acknowledged.

Notes

The authors declare no competing financial interest.

ACKNOWLEDGMENTS

This work was supported by the Russian Science Foundation (No. 19-73-00052). Physicochemical measurements were performed at Center for XRD Studies, Center for Optical and Laser Materials Research, and Center for Chemical Analysis and Materials Research (all belonging to Saint Petersburg State University). V.Y.K. thanks South Ural State University (Contract No. 02.A03.21.0011) for putting facilities at his disposal.

REFERENCES

- (1) Wang, W.; Zhang, Y.; Jin, W. J. Halogen bonding in room-temperature phosphorescent materials. *Coord. Chem. Rev.* **2020**, *404*, 213107.
- (2) Huang, Y.; Wang, Z.; Chen, Z.; Zhang, Q. Organic Cocrystals: Beyond Electrical Conductivities and Field-Effect Transistors (FETs). *Angew. Chem., Int. Ed.* **2019**, *58* (29), 9696–9711.
- (3) Sun, L.; Wang, Y.; Yang, F.; Zhang, X.; Hu, W. Cocrystal Engineering: A Collaborative Strategy toward Functional Materials. *Adv. Mater.* **2019**, *31* (39), 1902328.
- (4) Sun, L.; Zhu, W.; Yang, F.; Li, B.; Ren, X.; Zhang, X.; Hu, W. Molecular cocrystals: design, charge-transfer and optoelectronic functionality. *Phys. Chem. Chem. Phys.* **2018**, *20* (9), 6009–6023.
- (5) Bolton, O.; Lee, K.; Kim, H.-J.; Lin, K. Y.; Kim, J. Activating efficient phosphorescence from purely organic materials by crystal design. *Nat. Chem.* **2011**, *3* (3), 205–210.
- (6) Sivchik, V. V.; Solomatina, A. I.; Chen, Y.-T.; Karttunen, A. J.; Tunik, S. P.; Chou, P.-T.; Koshevoy, I. O. Halogen Bonding to Amplify Luminescence: A Case Study Using a Platinum Cyclometalated Complex. *Angew. Chem., Int. Ed.* **2015**, *54* (47), 14057–14060.

- (7) Sivchik, V.; Sarker, R. K.; Liu, Z.-Y.; Chung, K.-Y.; Grachova, E. V.; Karttunen, A. J.; Chou, P.-T.; Koshevoy, I. O. Improvement of the Photophysical Performance of Platinum-Cyclometalated Complexes in Halogen-Bonded Adducts. *Chem. - Eur. J.* **2018**, *24* (44), 11475–11484.

- (8) Yan, D.; Delori, A.; Lloyd, G. O.; Frisčić, T.; Day, G. M.; Jones, W.; Lu, J.; Wei, M.; Evans, D. G.; Duan, X. A Cocrystal Strategy to Tune the Luminescent Properties of Stilbene-Type Organic Solid-State Materials. *Angew. Chem., Int. Ed.* **2011**, *50* (S2), 12483–12486.

- (9) Pang, X.; Wang, H.; Wang, W.; Jin, W. J. Phosphorescent π -Hole $\cdots\pi$ Bonding Cocrystals of Pyrene with Halo-perfluorobenzenes (F, Cl, Br, I). *Cryst. Growth Des.* **2015**, *15* (10), 4938–4945.

- (10) Hori, A.; Takatani, S.; Miyamoto, T. K.; Hasegawa, M. Luminescence from π - π stacked bipyridines through arene-perfluoroarene interactions. *CrystEngComm* **2009**, *11* (4), 567–569.

- (11) Khan, A.; Wang, M.; Usman, R.; Sun, H.; Du, M.; Xu, C. Molecular Marriage via Charge Transfer Interaction in Organic Charge Transfer Co-Crystals toward Solid-State Fluorescence Modulation. *Cryst. Growth Des.* **2017**, *17* (3), 1251–1257.

- (12) Li, L.; Wang, H.; Wang, W.; Jin, W. J. Interactions between haloperfluorobenzenes and fluoranthene in luminescent cocrystals from π -hole $\cdots\pi$ to σ -hole $\cdots\pi$ bonds. *CrystEngComm* **2017**, *19* (34), 5058–5067.

- (13) Rozhkov, A. V.; Krykova, M. A.; Ivanov, D. M.; Novikov, A. S.; Sinelshchikova, A. A.; Volostnykh, M. V.; Kononov, M. A.; Grigoriev, M. S.; Gorbunova, Y. G.; Kukushkin, V. Y. Reverse Arene Sandwich Structures Based upon π -Hole \cdots [M^{II}] ($d^8M = Pt, Pd$) Interactions, where Positively Charged Metal Centers Play the Role of a Nucleophile. *Angew. Chem., Int. Ed.* **2019**, *58* (13), 4164–4168.

- (14) Muetterties, E. L.; Bleeke, J. R.; Wucherer, E. J.; Albright, T. Structural, stereochemical, and electronic features of arene-metal complexes. *Chem. Rev.* **1982**, *82* (5), 499–525.

- (15) Brooks, J.; Babayan, Y.; Lamansky, S.; Djurovich, P. I.; Tsyba, I.; Bau, R.; Thompson, M. E. Synthesis and Characterization of Phosphorescent Cyclometalated Platinum Complexes. *Inorg. Chem.* **2002**, *41* (12), 3055–3066.

- (16) Wu, W.; Wu, W.; Ji, S.; Guo, H.; Zhao, J. Accessing the long-lived emissive 3IL triplet excited states of coumarin fluorophores by direct cyclometallation and its application for oxygen sensing and upconversion. *Dalton Transactions* **2011**, *40* (22), 5953–5963.

- (17) Yan, Y.; Yu, Z.; Liu, C.; Jin, X. Effects of phenyl/thienyl substituents at acetylacetonate auxiliary ligands on the properties of cyclometalated platinum(II) complexes. *Dyes Pigm.* **2020**, *173*, 107949.

- (18) Laskar, I. R.; Hsu, S.-F.; Chen, T.-M. Highly efficient orange-emitting OLEDs based on phosphorescent platinum(II) complexes. *Polyhedron* **2005**, *24* (8), 881–888.

- (19) Johnson, E. R.; Keinan, S.; Mori-Sánchez, P.; Contreras-García, J.; Cohen, A. J.; Yang, W. Revealing Noncovalent Interactions. *J. Am. Chem. Soc.* **2010**, *132* (18), 6498–6506.

- (20) Contreras-García, J.; Johnson, E. R.; Keinan, S.; Chaudret, R.; Piquemal, J.-P.; Beratan, D. N.; Yang, W. NCIPLLOT: A Program for Plotting Noncovalent Interaction Regions. *J. Chem. Theory Comput.* **2011**, *7* (3), 625–632.

- (21) Reed, A. E.; Curtiss, L. A.; Weinhold, F. Intermolecular interactions from a natural bond orbital, donor-acceptor viewpoint. *Chem. Rev.* **1988**, *88* (6), 899–926.

- (22) Mou, X.; Wu, Y.; Liu, S.; Shi, M.; Liu, X.; Wang, C.; Sun, S.; Zhao, Q.; Zhou, X.; Huang, W. Phosphorescent platinum(ii) complexes containing different β -diketonate ligands: synthesis, tunable excited-state properties, and their application in bioimaging. *J. Mater. Chem.* **2011**, *21* (36), 13951–13962.

- (23) Li, K.; Ming Tong, G. S.; Wan, Q.; Cheng, G.; Tong, W.-Y.; Ang, W.-H.; Kwong, W.-L.; Che, C.-M. Highly phosphorescent platinum(ii) emitters: photophysics, materials and biological applications. *Chemical Science* **2016**, *7* (3), 1653–1673.

(24) Tekarli, S. M.; Cundari, T. R.; Omary, M. A. Rational Design of Macrometallo-cyclic Trinuclear Complexes with Superior π -Acidity and π -Basicity. *J. Am. Chem. Soc.* **2008**, *130* (5), 1669–1675.

(25) Mohamed, A. A.; Rawashdeh-Omary, M. A.; Omary, M. A.; Fackler, J. P., Jr. External heavy-atom effect of gold in a supramolecular acid–base π stack. *Dalton Transactions* **2005**, No. 15, 2597–2602.

(26) Elbjeirami, O.; Rashdan, M. D.; Nesterov, V.; Rawashdeh-Omary, M. A. Structure and luminescence properties of a well-known macrometallo-cyclic trinuclear Au(I) complex and its adduct with a perfluorinated fluorophore showing cooperative anisotropic supra-molecular interactions. *Dalton Transactions* **2010**, 39 (40), 9465–9468.

(27) Rawashdeh-Omary, M. A.; Omary, M. A.; Fackler, J. P.; Galassi, R.; Pietroni, B. R.; Burini, A. Chemistry and Optoelectronic Properties of Stacked Supramolecular Entities of Trinuclear Gold(I) Complexes Sandwiching Small Organic Acids. *J. Am. Chem. Soc.* **2001**, *123* (39), 9689–9691.

(28) Liu, J.; Yang, C.-J.; Cao, Q.-Y.; Xu, M.; Wang, J.; Peng, H.-N.; Tan, W.-F.; Lü, X.-X.; Gao, X.-C. Synthesis, crystallography, phosphorescence of platinum complexes coordinated with 2-phenyl-pyridine and a series of β -diketones. *Inorg. Chim. Acta* **2009**, *362* (2), 575–579.

(29) Sheldrick, G. M. Crystal structure refinement with SHELXL. *Acta Crystallogr., Sect. A: Found. Crystallogr.* **2008**, *A64*, 112–122.

(30) Frisch, M. J.; Trucks, G. W.; Schlegel, H. B.; Scuseria, G. E.; Robb, M. A.; Cheeseman, J. R.; Scalmani, G.; Barone, V.; Petersson, G. A.; Nakatsuji, H.; Li, X.; Caricato, M.; Marenich, A. V.; Bloino, J.; Janesko, B. G.; Gomperts, R.; Mennucci, B.; Hratchian, H. P.; Ortiz, J. V.; Izmaylov, A. F.; Sonnenberg, J. L.; Williams Ding, F.; Lipparini, F.; Egidi, F.; Goings, J.; Peng, B.; Petrone, A.; Henderson, T.; Ranasinghe, D.; Zakrzewski, V. G.; Gao, J.; Rega, N.; Zheng, G.; Liang, W.; Hada, M.; Ehara, M.; Toyota, K.; Fukuda, R.; Hasegawa, J.; Ishida, M.; Nakajima, T.; Honda, Y.; Kitao, O.; Nakai, H.; Vreven, T.; Throssell, K.; Montgomery, J. A., Jr.; Peralta, J. E.; Ogliaro, F.; Bearpark, M. J.; Heyd, J. J.; Brothers, E. N.; Kudin, K. N.; Staroverov, V. N.; Keith, T. A.; Kobayashi, R.; Normand, J.; Raghavachari, K.; Rendell, A. P.; Burant, J. C.; Iyengar, S. S.; Tomasi, J.; Cossi, M.; Millam, J. M.; Klene, M.; Adamo, C.; Cammi, R.; Ochterski, J. W.; Martin, R. L.; Morokuma, K.; Farkas, O.; Foresman, J. B.; Fox, D. J. *Gaussian 16, Rev. A.03*; Gaussian: Wallingford, CT, 2016.

(31) Boys, S. F.; Bernardi, F. The calculation of small molecular interactions by the differences of separate total energies. Some procedures with reduced errors. *Mol. Phys.* **1970**, *19* (4), 553–566.

(32) Rappoport, D.; Furche, F. Property-optimized Gaussian basis sets for molecular response calculations. *J. Chem. Phys.* **2010**, *133* (13), 134105.

(33) Weigend, F.; Ahlrichs, R. Balanced basis sets of split valence, triple zeta valence and quadruple zeta valence quality for H to Rn: Design and assessment of accuracy. *Phys. Chem. Chem. Phys.* **2005**, *7* (18), 3297–3305.

(34) Perdew, J. P.; Burke, K.; Ernzerhof, M. Generalized Gradient Approximation Made Simple. *Phys. Rev. Lett.* **1996**, *77* (18), 3865–3868.

(35) Perdew, J. P.; Ernzerhof, M.; Burke, K. Rationale for mixing exact exchange with density functional approximations. *J. Chem. Phys.* **1996**, *105* (22), 9982–9985.

(36) Grimme, S. Semiempirical GGA-type density functional constructed with a long-range dispersion correction. *J. Comput. Chem.* **2006**, *27* (15), 1787–1799.

(37) Grimme, S.; Antony, J.; Ehrlich, S.; Krieg, H. A consistent and accurate ab initio parametrization of density functional dispersion correction (DFT-D) for the 94 elements H-Pu. *J. Chem. Phys.* **2010**, *132* (15), 154104.